Interaction of Tip Vortices Generated by a Split Wing

Won Suk Youn*, Yong Oun Han and Dong Yeon Lee****
School of Mechanical Engineering
Yeungnam University, Gyongsan, Korea 712-749

Abstract

To reduce the strength of tip vortex of the fixed wing, a horizontal wing-let splitted into two parts was utilized, and the interaction between vortices generated by these wing-lets was investigated by the hot-wire anemometry. The process of vortex forming and merging was clarified by measurements of velocity vectors and their contours at five downstream cross-sections; 0.05C(chord length), 0.2C, 0.5C, 1.0C and 2.0C. Both vortex-lets formed by each wing-lets rotate counterclockwise and merge into a larger single vortex within a short downstream distance, 0.5C in this case. The strength of the merged tip vortex turned out to become smaller than that of the plain wing tip near the vortex core.

Key Word : split wing, wing-let, merged vortex, vortex strength, hot-wire anemometry

Introduction

From the aerodynamic view point a trailing vortex frequently brings about disadvantages such as an increase of profile drag, air-traffic limits at take-off/landing, the vortex-airframe interaction to cause a severe noise and vibration, and so on. It is inevitable for the finite wing to generate the tip vortex by the pressure discontinuity between upper and lower surfaces at the tip, i.e., the 3-dimensional effect. Although the tip vortex is to be unavoidable, its strength can be reduced by proper aerodynamic devices. If there is any flexible device to adjust the pressure difference at the tip, it will minimize the vortex strength. Typical devices to reduce the vortex strength intend conceptually to improve the flexibility of the fixed wing tip as far as they have the sufficient stiffness like a bird wing.

Researchers have made efforts to modify the vortex structures of the plane wing and reduce their strengths. Since most tip vortices are fairly dependent on the initial conditions, it is most effective to change the geometric configuration of the wing tip, as in the wing-lets[1, 2], but this device frequently increases an aerodynamic load at the tip. Without any geometric modifications of the wing tip, it has been tried to reduce the vortex strength by the boundary layer controls near the tip[3, 4]. To reduce the tangential velocity component of the tip vortex the porous wing with the vertical holes was used. The porous wing allows some of the high-pressure-air on the lower surface to blow to the upper surface.

Unfortunately, most of these results bring about the other penalties such as increase of drags by the associated geometric changes while they have successes to reduce strengths. To solve this problem, slotted wing experiments[5, 6] were done and showed some advantages to reduce the strength with the minimum penalty. These results concluded that the slotted wing was able to exclude the formation of the secondary vortex at the vertical tip face. Therefore, it

* Graduate Student
** Professor
E-mail : yohan@yu.ac.kr, TEL : 053-810-2454, FAX : 053-813-3703

is conjectured that the formation of the trailing vortex is closely correlated to the communication between the sub-vortices around the vertical tip face. The roll-up structure is strongly dependent on several parameters; tip shape, the angle of attack, aspect ratio, Reynolds number, and so on. Roll-up structure has been observed by the flow visualizations in the previous works[7-11].

Another interesting phenomenon in the vortex structure is the acceleration of the axial velocity component. Similar results were reported in the works [12, 13]. Recently, Bae and Han[14] carried out the LDV measurement to unveil the velocity vectors along the sequential vertical planes to the virtual vortex trail even before the trailing edge. It was found that when the roll-up progresses with sub-vortices near the tip, there exists a sudden negative pressure zone near the virtual center of the premature vortex and this allows the axial velocity to accelerate, being faster than the inflow velocity. Therefore, to understand the interaction between sub-vortices generated at different local area on the same wing is the shortcut to provide a way to control the vortex strength.

Another interesting tip shape can be observed at the bird wing. The bird wing has many splits at the tip with their abundant flexibilities. When the bird cruises and flutters its wing splits into many parts, making many tiny vortex-lets at its wing posture by minimizing the energy loss. Comparing to the energy consumed by one large vortex of the typical plane wing, it is presumable that the integration of energy consumed by total tiny vortex-lets generated by the bird wing be much smaller. With these observations bird exactly has both characteristics; flexibility of each feather and split of wings, maintaining the proper wing geometry. In this paper as the first step to apply the split wing of a bird to the typical plane, a simple split wing of two horizontal wing-lets will be utilized and confirmed to establish another device to reduce the vortex strength.

Experiment

Experiment was carried out through a blow down wind tunnel which has the test section of 0.9 x 0.7 x 1.8(m), contraction ratio of 6:1 to the settling chamber, turbulent intensity of 0.5% at the inlet of test section. The flow was generated by an axial type blower with diameter of 1.8m and 37kW AC motor. A straight NACA23012 airfoil section with the chord of 0.15m and the span of 0.45m fabricated the half wing. Two horizontal wing-lets which have the same planform area of span of 0.05m and chord of 0.075m, and also have NACA23012 profile, were mounted at the vertical main wing tip. Both wing-lets can vary their angle of attack at 1/4 wing-let chords respectively(see the schematic drawing in Fig. 1). To obtain the optimized wing-let postures which can show effectively the interaction between vortices generated by each wing-lets tremendous amount of visualizations using smoke and Laser sheet have been done as shown in Fig. 2.

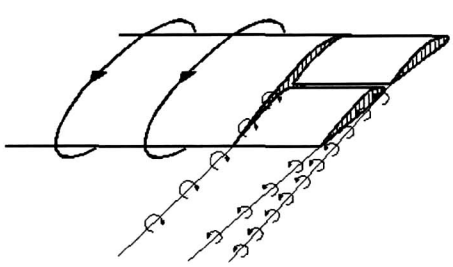

Fig. 1. Split Wing geometry

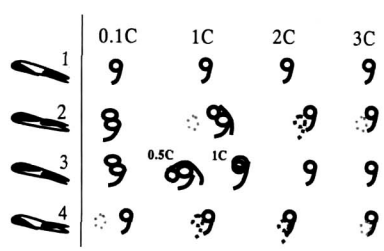

Fig. 2. Vortices Formations Generated by Split Wing

Fig. 2 shows schematics of visualization results for four different arrangements of wing-lets. The angle of attack of the main wing was fixed at 8° . For the case 1, both the front and the rear winglets were set at the same angles of attack, 8° . And the case 2 has the arrangement of 6° and 8° for the front and the rear, respectively. 6° and 10° were for the case 3, and 10° and 8° were for the case 4. During the smoke visualization, the case 3 gave the best picture to observe merging process between two vortices made by both wing-lets. Hereafter, all measurements were carried out only in the case 3.

The X-wire sensor was built from 5 μm diameter of tungsten wire and each ends were copper plated at the prong, giving the effective length to diameter ratio of 120 for each wire. Outputs of X-wire were amplified by two CTA system with the over heat ratio of 1.6, and low-pass filtered at 2kHz. The dynamic analog signals were digitized by the 16-bit A/D converter and stored in Pentium PC. Wire calibration was carried out by the fourth order polynomial rules[15] and the coefficients of angle calibration were 0.2 and 0.4, respectively. Measurement volumes were selected to capture the vortex and vortex-lets in the same frame on the vertical plane to the vortex trail. To obtain the target volume several preliminary tests were carried out. Once the target frame was selected, we put 289 data points with 3mm square grids within 0.05 x 0.05(m) square plane. To obtain the historical or, evolving process of vortices, five downstream positions were selected at 0.05C, 0.2C, 0.5C, 1.0C and 2.0C. A three-dimensional traversing unit that has the spatial resolution of 0.2mm and controlled by D/A inputs was used to position the sensor.

To obtain the independent sampled data, data were sampled at 100Hz and 1000 data was used to satisfy the 0.3% converging criteria[16]. To obtain three velocity components at every point two sets of X-wire measurements were carried out with velocity pairs; UV and UW, respectively. The maximum discrepancy in U reading between the two set of experiments gave the error bound of 4.3%. Therefore, including the possible error from the hot wire calibration, the accuracy of the mean data has about 5% of the accumulated error bound through whole experiments.

Results and Discussions

To examine the merging mechanism, five measurement volumes were selected in the range from 0.02C to 2.0C. The results are shown in Fig. 3 for the axial velocity contours and in Fig. 4 for the vertical velocity components. Fig. 3 shows how vortices evolve downstream. The velocity deficit of the axial velocity component take place behind the wing span and near the vortex core. As shown in the section of 0.05C, tip vortex generated by the front wing-let places at upper left side from the tip edge when that of the rear wing-let starts to generate at the edge. Also, it can be seen at the section of 0.2C that the rear vortex separates from the tip and starts to roll up counterclockwise. Trails of both vortex centers are getting closer in downstream while rotating helically and merge into a single big vortex at 0.5C. The corresponding vector plots of vertical velocities are also given in Fig. 4, which explain this merging process as well. This evolving process was also observed in the smoke visualization as aforementioned. This merged single vortex drifts, for a while, maintaining the substantial amount of angular momentum and its core grows with downstream distance. Fig. 5 shows the superposition of both plots at 2.0C, where the tip vortex is reported to grow sufficiently as seen in previous results. Data obtained at 2.0C will be analyzed to see how the vortex strength of split wing changes, compared to that of the plain wing.

To investigate vortex structure in detail, three component velocities have been measured along the horizontal axes containing both vortex cores in the earlier sections. The axes are noted as AA′, BB′, CC′, DD′ and EE′, respectively in Figs. 4 and 5. These results are plotted in Fig. 6 for the axial velocity components. Considering the fact that the typical single vortex tends to have Gaussian profile for the axial component, it seems that two small vortices are present at planes, 0.05C and presumably 0.2C, based on their peaky profiles. After 0.5C there show off only single-peaks with approximate Gaussian profiles. This convinces that the merging process became complete. Merging

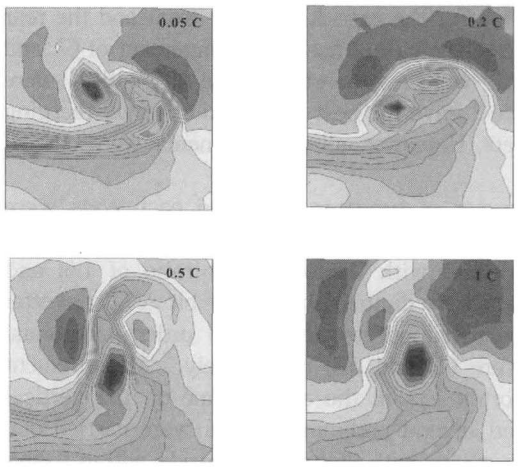

Axial velocity contour around the wing tip near field

Fig. 3. Contour Plot of Axial Velocity
(a)0.05C (b)0.2C (c)0.5C (d)1.0C

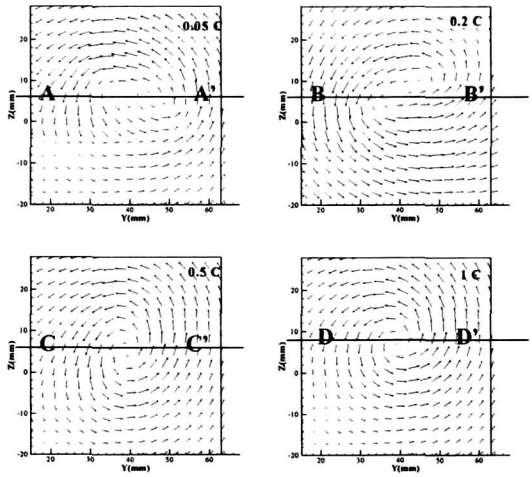

Fig. 4. Vector Plot of Vertical Velocity
(a)0.05C (b)0.2C (c)0.5C (d)1.0C

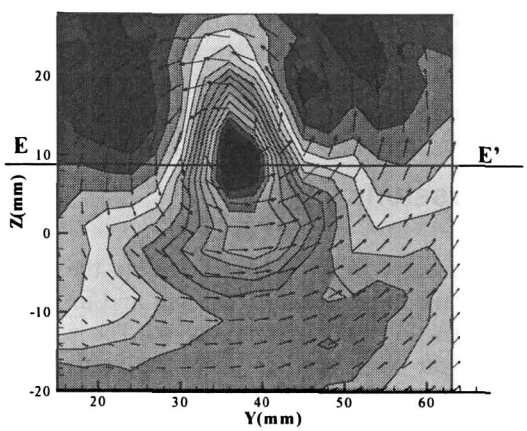

Fig. 5. VW Velocity vector and U contour of the wing around the tip vortex core at vertical cross section(x=2C)

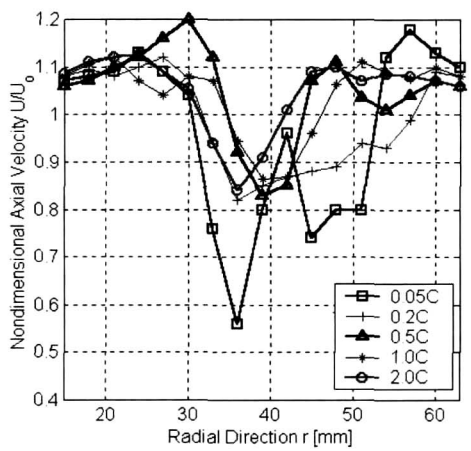

Fig. 6. Axial Velocity along Radial Direction

step is also observed in the sequential profiles of the swirl components of Fig. 7. The peaky shapes near the core center are brought about by two small vortices. As they go downstream there appears the merged single vortex maintaining the point symmetric profile at the core center after 0.5C. As shown in Fig.s 6 and 7, it convinces the fact that the merged single vortex appears after 0.5C while two small vortices are shown off in the earlier sections, 0.05C and 0.2C.

Observing the sequential profiles in both figures, peak values become smaller with downstream distance once a single vortex is established at 0.5C. It is known that swirl strength starts decaying at the plane of 1.0C for the typical trailing vortex. The turbulent kinetic energy(TKE) is defined as

$$q^2 = \frac{1}{2}(u'^2 + v'^2 + w'^2) / U_o^2 \qquad (1)$$

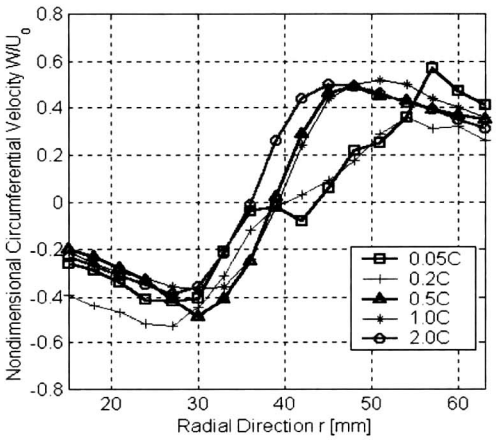

Fig. 7. Circumferential Velocity along Radial Direction

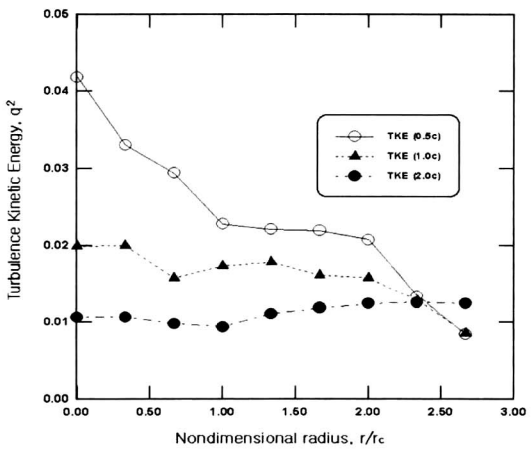

Fig. 8. Turbulent Kinetic Energy

q^2 distributions are plotted in Fig. 8 at 0.5, 1.0 and 2.0C. The TKE at vortex centers decays rapidly with downstream distance, and becomes flat in the radial direction. It implies that the axial component of the total mean kinetic energy obtained by the tip transfers within a short time period into the swirl kinetic energy as it goes downstream.

In order to compare the present results to those of the plain wing and the rotor, swirl velocities measured at 2.0C were used. The distribution of W(r) at 2.0C is found to agree best with the model profile of the typical single vortex. For the swirl velocity there are known several models including Vatistas' algebraic model[17] described as

$$\overline{W}(\overline{r}) = \frac{\overline{r}}{[1+(\overline{r}^{2n})]^{1/n}}, \quad \overline{r} = r/r_c \tag{2}$$

where W is the normalized swirl velocity by the mean axial component, U in upstream and r_c means the radius of the vortex core. It reports that the swirl velocity profile of the tip vortex generated by the plain fixed wing is fit to n=1 while that of the rotor is fit to n=2 model, respectively[14]. But, the present vortex of this split wing shows the best curve fit at n=0.8 as shown in Fig. 9.

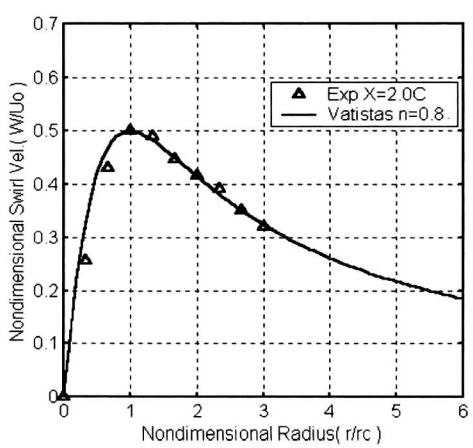

Fig. 9. Swirl Velocity at 2.0C and Best Fitting Curves with Vatistas Model

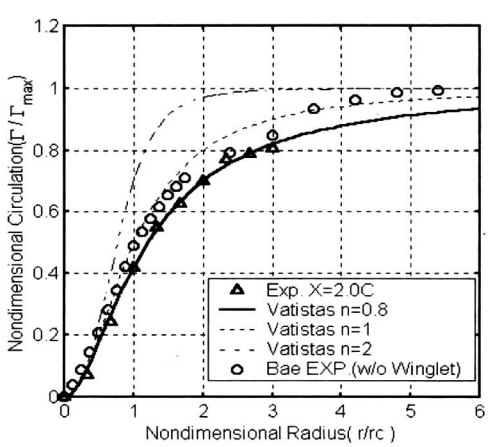

Fig. 10. Comparison of Nondimensional Circulation w/ and w/o Winglets

The profile of circulation explains how the tip vortex is constructed along the radial direction. It can also analyze how the core action leads the energy transportation from the center to the core boundary and over the far field. For this purpose circulations are calculated by use of the following equation[14] with measured swirl velocities at every radial distance;

$$\Gamma(r) = \oint \vec{V} \cdot \vec{ds} = W(r) \cdot 2\pi r \tag{3}$$

To compare the split case to the others, the circulation evaluated by the above equation is plotted in Fig. 10. The circulation is normalized by the maximum circulation, which was chosen at 20 nondimensional radii as for the farthest location in Fig. 9. Over further distance the nondimensional swirl velocity establishes the convergency. The circles show the circulation distributions of the slotted wing measured by Bae and Han[14], and the lines show Tung's model [18] values, respectively. Comparing these results, the strength of split wing tip vortices become weaker than that of the slotted wing. The fact that near the center the split wing generates weak vortices suggests that splitting the wing tip geometry in spanwise direction like the bird wing can be applied as a device to weaken the vortex strength at the tip.

Conclusions

The weak tip vortex of the front wing-let was merged into that of the rear vortex. The merging process has been completed at the plane of 0.5C based on profiles of axial and swirl velocity components. Both vortices have spiral trails rotating counterclockwise and merged. The strength of the merged vortex resulted by two vortices become weaker than that of the plain vortex. It implies that the split wing can be a device to weaken tip vortex.

Acknowledgement

This work has been supported by Yeungnam University Research Grant 99, which authors greatly acknowledge. And the partial support of BK21 is also acknowledged.

References

1. Mueller, R.H. and Staufenbiel, R., 1987, "The Influence of Winglets on Rotor Aerodynamics", *Vertica*, Vol. 11, No. 4, pp. 601~618.

2. Marchman III, J. F. and Uzel, J. N., 1972, "Effect of Several Wing Tip Modifications of a Trailing Vortex", *J. of Aircraft Engineering Notes*, Vol. 9, No. 9, pp. 684~686.

3. Perry, F.J., 1989, "The contribution of planform area to the performance of the BERP rotor", *Journal of AHS*, January, pp. 64-66.

4. Ghee, T.A. and Leishman, J.G., 1992, "Unsteady circulation control aerodynamics of a circular cylinder with periodic jet blowing", *AIAA Journal*, Vol. 30, No. 2, February, pp.10-18.

5. Chow, J.S., Zilliac, G.G. and Bradshaw, P., 1997, "Mean and turbulence measurements in the near field of a wing tip vortex", *AIAA Journal*, Vol. 35, No. 10, pp.1561-1567.

6. Chiger, N.A. and Corsiglia, V.R., 1971, *Tip vortices-velocity distribution*, NASA TM. X-62087, September.

7. Thompson, D.H., 1975, " Experimental Study of Axial Flow in Wing Tip Vortices", *J. Aircraft*, Vol.12, No. 11, pp. 910~911.

8. Francis, T.B. and Katz, J., 1988, "Observations on the Development of a Tip Vortex on a Rectangular Hydrofoils", *Transactions of the ASME*, Vol. 110, No. 2, pp. 208~215

9. Katz, J. and Bueno Galdo, J., 1989, "Effect of roughness on Roll-up of Tip Vortices on a

Rectangular Hydrofoil", *J. of Aircraft*, Vol. 26, No. 3, March, pp. 247~253.

10. Engel, M.A. and Davenport, W.J., 1995, "A Wind Tunnel Investigation of a Wing-Tip Trailing Vortex", *VPI-AOE-218*, VPI&SU, Blacksburg, VA.

11. Han, Y.O., Leisman, J.G. and Coyne, A.J., 1996, "On the Turbulent Structure and Development of a Wing-Tip Vortex", *JFM*, Vol. 312, pp. 67~106.

12. Bae, H and Han, Y.O., 1998, "Deformation of Tip Vortex Generated by a Fixed Wing with Slot", *Proc. of 1998 Autumn Meeting*, KSAS, pp. 120~123. (Korean)

13. Han, Y.O. and Bae, H., 1999, "Modification of tip vortex by spanwise slots", KASA Journal, Vol. 27, No. 5, pp.1-7.

14. Bae, H. and Han, Y.O., 1999, "Roll-up structure of tip vortices along the flat tip face of an half wing", *Proc. of the first joint symposium between Hokkaido Univ. and Yeungnam Univ.*, Gyongsan, Korea, pp. 25~29.

15. George, W.K., 1987, "The decay of homogeneous isotropic turbulence", *Proc. of 2nd International Turbulence Conference*, Tokyo University, Japan.

16. George, W.K., 1978, "Processing of random signals," *Proceedings of the Dynamic Flow Conference*, pp.757-793.

17. Vatistas, G.H., Kozel,V., Mih, W.C., 1991, "A Simpler Model for Concentrated Vortices", *Experiments in Fluids*, Vol. 11, pp. 73~76.

18. Tung, C., Pucci, S.L., Caradonna, F.X. and Morse, H.A., 1983, "The structure and trailing vortices generated by model rotor blades", *Vertica*, Vol. 7, pp.33~43.